Virology 462-463 (2014) 318–327

Contents lists available at ScienceDirect

Virology

journal homepage: www.elsevier.com/locate/yviro

Factors affecting *de novo* RNA synthesis and back-priming by the respiratory syncytial virus polymerase

Sarah L. Noton [a], Waleed Aljabr [b], Julian A. Hiscox [b,c], David A. Matthews [d], Rachel Fearns [a,*]

[a] Department of Microbiology, Boston University Medical Campus, 72 East Concord Street, Boston, MA 02118, USA
[b] Department of Infection Biology, Institute of Infection and Global Health, University of Liverpool, ic2 Building, Liverpool L3 5RF, UK
[c] NIHR Health Protection Research Unit in Emerging and Zoonotic Infections, University of Liverpool, ic2 Building, Liverpool L3 5RF, UK
[d] School of Cellular and Molecular Medicine, University of Bristol, Bristol BS8 1TD, UK

ARTICLE INFO

Article history:
Received 6 May 2014
Returned to author for revisions
20 May 2014
Accepted 30 May 2014
Available online 8 July 2014

Keywords:
Respiratory syncytial virus
Paramyxovirus
Mononegavirales
RNA dependent RNA polymerase
Back-priming
RNA synthesis

ABSTRACT

Respiratory syncytial virus RNA dependent RNA polymerase (RdRp) initiates RNA synthesis from the *leader* (*le*) and *trailer-complement* (*trc*) promoters. The RdRp can also add nucleotides to the 3′ end of the *trc* promoter by back-priming, but there is no evidence this occurs at the *le* promoter in infected cells. We examined how environmental factors and RNA sequence affect *de novo* RNA synthesis *versus* back-priming using an *in vitro* assay. We found that replacing Mg^{2+} with Mn^{2+} in the reaction buffer increased *de novo* initiation relative to back-priming, and different lengths of *trc* sequence were required for the two activities. Experiments with *le* RNA showed that back-priming occurred with this sequence *in vitro*, but less efficiently than with *trc* RNA. These findings indicate that during infection, the RdRp is governed between *de novo* RNA synthesis and back-priming by RNA sequence and environment, including a factor missing from the *in vitro* assay.

Introduction

Respiratory syncytial virus (RSV), a significant cause of severe acute lower respiratory disease (Nair et al., 2010), belongs to the family *Paramyxoviridae* in the order *Mononegavirales*. Members of this order of viruses have a single stranded, negative sense RNA genome, which is transcribed and replicated by the viral RNA dependent RNA polymerase (RdRp). In comparison to the RdRps of positive and double stranded RNA viruses, which have been extensively studied, very little is known about the RdRps of negative strand RNA viruses, and in particular the non-segmented negative strand (NNS) RNA viruses.

Like other NNS RNA viruses, the RSV RdRp initiates RNA synthesis from two promoters: the leader (*le*) promoter that lies at the 3′ end of the genome RNA, which signals initiation of mRNA transcription and RNA replication, and the trailer complement (*trc*) promoter that lies at the 3′ end of the replicative intermediate RNA, the antigenome, which signals synthesis of RNA replication to produce genome RNA (Cowton et al., 2006). Recent studies have shown that the RSV RdRp has complex activities at the promoters, and in particular, at the *trc* promoter. It can initiate RNA synthesis at positions +1 and +3 of both the *le* and *trc* promoters (Fig. 1A) (Noton et al., 2010, 2012; Noton and Fearns, 2011; Tremaglio et al., 2013). In addition, it can extend the 3′ terminus of *trc* RNA using a back-priming mechanism in which the RNA folds into a secondary structure and the RdRp adds predominantly G, GU, or GUC using the internal RNA sequence as a template (Noton et al., 2012) (Fig. 1B). In infected cells, this leads to a heterogeneous population of *trc*-containing RNA, with approximately 40% of transcripts modified by 3′ extension. In contrast, there was no evidence for 3′ modification of *le* containing RNA isolated from infected cells (Noton et al., 2012). The significance of 3′ extension at the *trc* promoter is unknown, but in the context of naked RNA, the additional nucleotides inhibit promoter activity, suggesting that 3′ extension may represent a mechanism by which the activity of the *trc* promoter is regulated.

The finding that the RdRp could perform back-priming on *trc* RNA was surprising because NNS RNA virus replicative RNA is encapsidated with nucleoprotein (N) throughout infection. Atomic structures of N–RNA complexes from several NNS RNA viruses, including RSV, suggest that encapsidated RNA would be devoid of secondary structure (Albertini et al., 2006; Bakker et al., 2013; Green et al., 2006; Tawar et al., 2009). However, the finding that back-priming at the *trc* promoter can occur in RSV infected cells indicates that this promoter containing RNA can adopt a secondary

* Corresponding author. Tel.: +1 617 638 4034, fax: +1 617 638 4286.
E-mail addresses: slnoton@bu.edu (S.L. Noton), w.aljabr@liverpool.ac.uk (W. Aljabr), julian.hiscox@liverpool.ac.uk (J.A. Hiscox), d.a.matthews@bristol.ac.uk (D.A. Matthews), rfearns@bu.edu (R. Fearns).

http://dx.doi.org/10.1016/j.virol.2014.05.032
0042-6822/

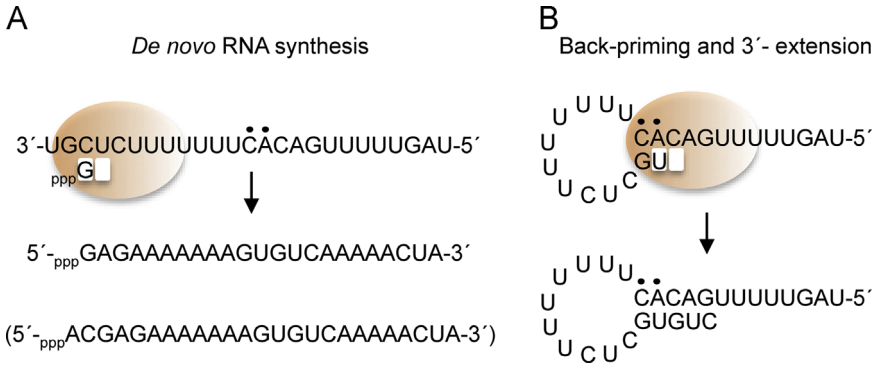

Fig. 1. Different configurations of the RdRp and RNA at the *trc* promoter. (A, B) The 3′ 25 nt of the *trc* promoter region, which correlate with the RNA template used previously in reconstituted RNA synthesis assays (Noton et al., 2012), are shown. Nucleotides 13 and 14, which are involved in back-priming, are indicated with black dots. The RdRp is shown as a shaded oval, with the priming and incoming nucleotide sites shown as white boxes. (A) Orientation and positioning of the RdRp relative to the *trc* RNA for *de novo* RNA synthesis from position +3 of the *trc* promoter. The arrow points to the full-length product that would be generated from this site in the *in vitro* assay. The RdRp can also initiate at position +1 to generate the product shown in parentheses, but the initiation mechanism has not been characterized. (B) Orientation of the RdRp and *trc* RNA for back-priming and 3′ extension, with nucleotides 13C and 14A base-paired with nucleotides 2G and 1U, respectively. The arrow points to the 28 nt product that is generated when the 3′ end of the RNA is extended by three nucleotides. In addition, in the *in vitro* assay, nucleotides 1 and 2 can base-pair with nucleotides 15 and 16, to prime addition of CTP to the 3′ end of the template RNA (not shown).

structure and so presumably is unencapsidated, at least some of the time, during infection. This finding is in keeping with other information obtained regarding RSV, including the fact that although each N monomer binds seven nt, the RSV genome nucleotide length is not divisible by seven, and in contrast to many other paramyxoviruses, RSV template activity is not sensitive to insertions and deletions that would disrupt any phasing that exists between N protein and the RNA (Kolakofsky et al., 2005; Samal and Collins, 1996). In addition, RNA probes have been shown to hybridize specifically to RSV genome RNA in infected cells (Jung et al., 2013; Lifland et al., 2012; Lindquist et al., 2010; Santangelo et al., 2009), indicating that there are occasions when some of the RNA is at least transiently exposed. Together, these observations lend support to the idea that the RSV promoters might not always be completely encapsidated during infection.

The ability of the RdRp to interact with *trc* to perform either *de novo* RNA synthesis or 3′ extension by back-priming indicates that it can engage the promoter in two completely different configurations (Fig. 1, compare A and B). Given that 3′ extension and *de novo* RNA synthesis involve the RdRp interacting with *trc* RNA in two different ways, it would be valuable to have a greater understanding of factors that influence RdRp activity when it encounters the *trc* sequence, and to determine if sequence differences between *le* and *trc* account for why *le* RNA is not modified by 3′ extension in RSV infected cells. Thus, the aim of the work described here was to examine how environment and RNA sequence affect RdRp activities at the promoter.

Results

Characterization of the products generated in an in vitro RNA synthesis assay

The *de novo* RNA synthesis and 3′ extension activities of the RSV RdRp were reconstituted in an *in vitro* RNA synthesis assay, described previously (Noton et al., 2012). Recombinant RSV RdRp, consisting of purified complexes of the large polymerase subunit (L) and phosphoprotein (P), was incubated with an RNA oligonucleotide consisting of nucleotides 1–25 of *trc* promoter sequence and all four NTPs, including [α^{32}P] GTP. As a negative control, RNA synthesis reactions were performed with a mutant RdRp, in which the L component of the RdRp contained an N812A mutation in the RNA synthesis catalytic site (Fig. 2A, lane 4), or the RdRp was omitted from the reaction (Fig. 2A, lane 3). Similarly to previously published results, wt RSV RdRp generated a number of transcripts (Fig. 2A, lane 5). Bands ≥26 nt represent products of 3′ extension (Noton et al., 2012). These bands typically appeared as a triplet of products 26, 27 and 28 nt in length, corresponding to addition of one, two or three nucleotides (see also Fig. 2D). Longer exposures also revealed smaller amounts of longer products of appropriate length of RNA generated by RdRp that engaged in back-priming, but extended to the end of the template (Fig. 2D, lane 10). The products of *de novo* RNA synthesis products appeared as a ladder of bands 6–25 nt in length with a dominant band at 21 nt. There were also dominant bands at 8 and 9 nt which likely represent abortive initiation products generated by RdRp that failed to escape the promoter (Fig. 2A, lane 5). As described in the *Introduction*, in infected cells the RSV RdRp initiates at the +1 and +3 sites on the *trc* promoter. To examine if this was the case in the *in vitro* assay, RNA synthesis reactions were performed either with [γ-^{32}P] ATP or [γ-^{32}P] GTP, rather than [α-^{32}P] GTP, to detect RNA initiated at +1U or +3C, respectively. Reactions containing [γ-^{32}P] ATP yielded products up to 25 nt in length, with dominant bands at 21–25 nt (Fig. 2B, lane 6). In contrast, reactions containing [γ-^{32}P] GTP yielded products up to 23 nt in length, with a dominant band at 21 nt (Fig. 2C, lane 6). These results confirmed that RNAs were initiated at +1 and +3, respectively, but RNA initiated from +1 could only be detected following long reaction times, and the signal was consistently weak, indicating that initiation from this site was relatively inefficient. Thus, bands characterized as *de novo* synthesized RNA include RNA transcripts initiated from +1 and +3, but with RNA initiated at +3 being dominant.

In the experiment shown in Fig. 2A, the 3′ extension bands are very strong compared to bands representing *de novo* RNA synthesis products. This was somewhat surprising given that it is believed the major function of the *trc* sequence is to direct initiation of *de novo* RNA synthesis, and RNA from infected cells showed that not all the *trc* RNA was modified by back-priming (Noton et al., 2012). To confirm that the high level of 3′ extension was not an artifact of extended incubation times, RNA synthesis reactions were incubated for varying lengths of time. This analysis showed that the products of *de novo* RNA synthesis and 3′ extension could both be detected following a 5 min incubation period, and that their ratios did not change over the timecourse (Fig. 2D, lanes 4–10; Fig. 2E). This was also the case if the reaction conditions were varied (data not shown). These data showed that

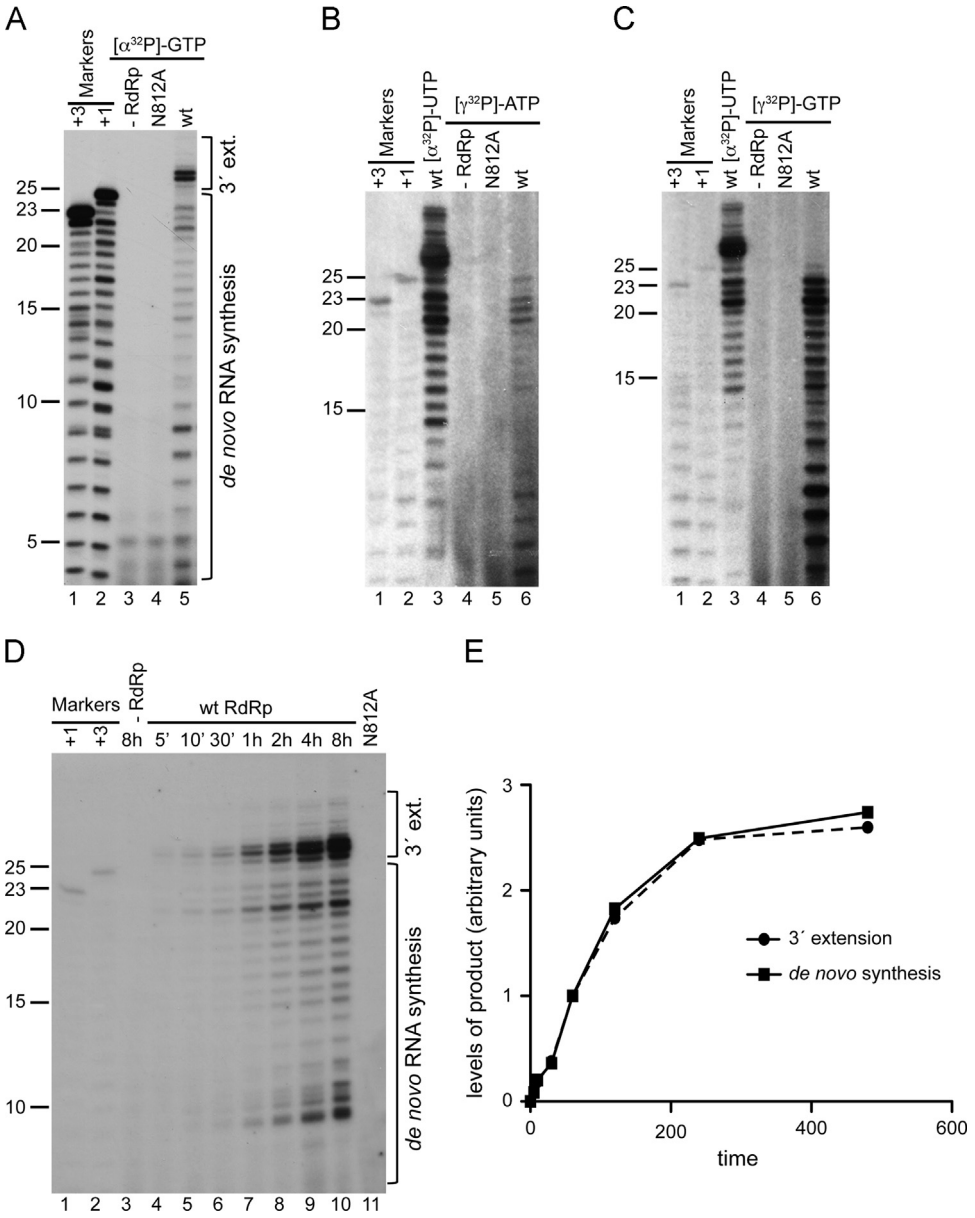

Fig. 2. Characterization of the products generated in an *in vitro* RNA synthesis assay. (A) Products of the RSV RdRp in an *in vitro* assay. The RSV RdRp was incubated for 3 h with a template representing nucleotides 1–25 of the *trc* promoter sequence in a buffer the same as standard reaction buffer, except that it contained 1 mM ATP, CTP and UTP and 250 μM GTP with [α-^{32}P] GTP. The products were migrated directly on a denaturing polyacrylamide gel. Lane 3 is a negative control in which the L/P complex was omitted from the reaction, and lane 4 is a negative control in which reactions were incubated with the L/P complex containing the N812A substitution at the catalytic site of the L protein. (B, C) *De novo* RNA synthesis involves initiation from the +1 and +3 sites. RSV RdRp was incubated for 6 h with a template representing nucleotides 1–25 of the *trc* promoter sequence in a buffer that was the same as the standard reaction buffer, except that the NTP concentrations were reduced to 500 μM each, supplemented with either [α-^{32}P] UTP (B, C, lane 3), [γ-^{32}P]ATP (B, lanes 4–6) or [γ-^{32}P]GTP (C, lanes 4–6). (D) Accumulation of RNA synthesis products over time. The RSV RdRp was incubated with a template representing nucleotides 1–25 of the *trc* promoter sequence in a standard reaction buffer, including [α-^{32}P] GTP, and incubated for the times indicated before heat inactivation of the RdRp. In panels A–D, lanes 1 and 2 contain size markers representing nt 3–25 or 1–25 of *tr*, the expected products of +3 and +1 *de novo* RNA synthesis, respectively. (E) Graph showing quantification of the RNA products shown in panel D. The 21 nt and 26–28 nt bands representing *de novo* RNA synthesis products and products of 3′ extension, respectively, were quantified. In each case, the values were normalized to the 1 h time point value, which was set to 1. This graph represents one of three independent experiments, each performed with slightly varied reaction conditions and time points.

the relative levels of 3′ extension and *de novo* RNA synthesis did not vary over time in the *in vitro* RNA synthesis assay.

3′ extension and de novo RNA synthesis are differentially affected by divalent cations

Metal cations are required for polymerization activity. They function to coordinate incoming NTPs and allow phosphoryl transfer (Yang et al., 2006). In most cases Mg^{2+}, which is abundant in cells and has stringent coordination requirements, is optimal. However, Mn^{2+}, which has a similar chemistry to Mg^{2+}, but relaxed coordination requirements, often can be used (Yang et al., 2006). Substituting Mg^{2+} with Mn^{2+} can alter RdRp structure and has been shown to have complex effects on the activities of viral RdRps (Arnold et al., 1999, 2004; Butcher et al., 2001; Palmenberg and Kaesberg, 1974; Ranjith-Kumar et al., 2002a, 2002b; Shim et al., 2002). In the case of the RSV RdRp, the first step in initiation at the promoter must involve polymerization of two NTPs (*de novo* initiation), whereas back-priming and 3′ extension involves nucleotide addition to the 3′ end of an existing RNA (Fig. 1). Studies with positive strand RNA viruses have shown that

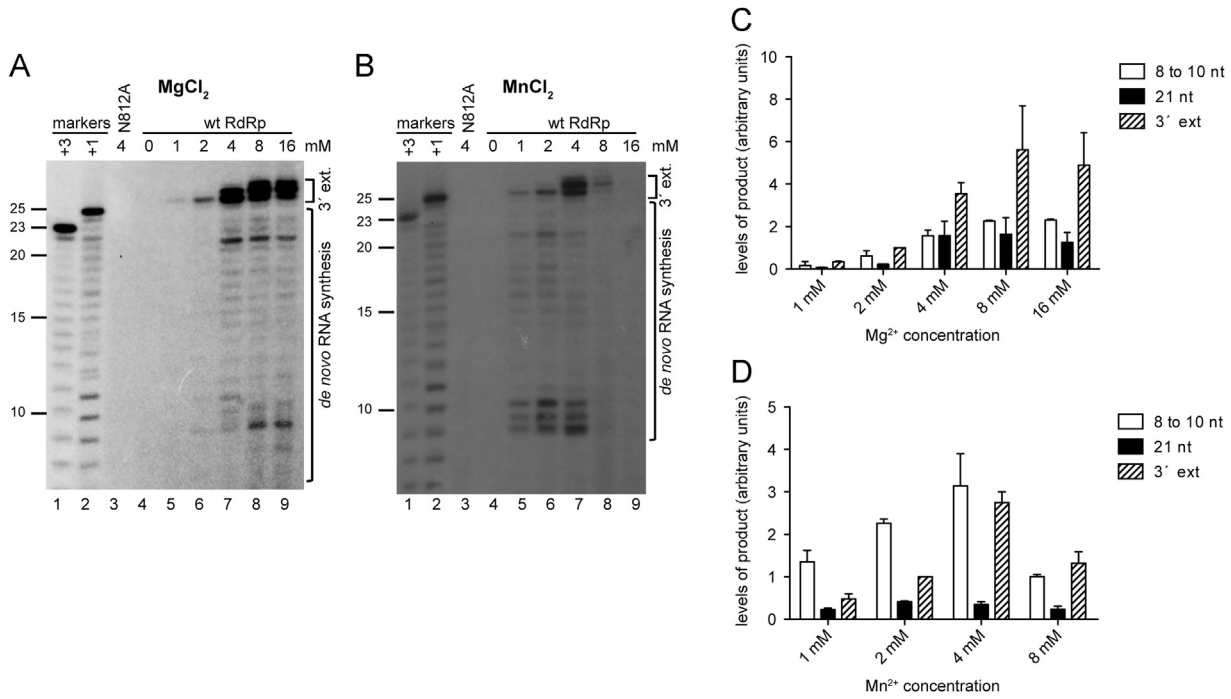

Fig. 3. Effect of Mg^{2+} and Mn^{2+} on the activities of the RSV RdRp. (A, B) 200 ng of L/P RdRp preparation was combined with a buffer similar to standard buffer, containing [α-^{32}P] GTP, but lacking glycerol, and with between 0 and 16 mM $MgCl_2$ or $MnCl_2$, as indicated. The template represented nucleotides 1–25 of the *trc* promoter sequence and reaction mixes was incubated for 2 h. RNA was analyzed by denaturing urea–acrylamide gel electrophoresis and autoradiography. Lanes 1 and 2 contain molecular weight ladders representing the expected products of *de novo* RNA synthesis from positions +3 and +1, respectively. Lane 3 is a negative control in which reactions were incubated with the L/P complex containing the N812A substitution at the catalytic site. (C, D) Bar charts showing levels of abortive initiation, elongation and 3′ extension products with different concentrations of Mg^{2+} (panel C) and Mn^{2+} (panel D). The 8–10 nt, 21 nt and 26–28 nt bands were quantified. The data show the mean and range of two independent experiments. The data from each experiment were normalized to 3′ extension at 2 mM, which was set to a value of 1. Note that no correction was made for the expected number of [α-^{32}P] GTP incorporation sites in each of the products, and that while the trends between the Mg^{2+} and Mn^{2+} bar charts can be directly compared, the absolute values cannot be.

substituting Mg^{2+} with Mn^{2+} can alter the relative efficiencies of *de novo versus* primed initiation (Arnold et al., 1999; Ranjith-Kumar et al., 2002b). Therefore, we examined if *de novo* RNA synthesis and 3′ extension were differentially affected by Mg^{2+} *versus* Mn^{2+}. In addition, the relative levels of short and long *de novo* RNA synthesis products were examined to determine if Mg^{2+} and Mn^{2+} had different effects on initiation *versus* elongation of *de novo* synthesized RNA.

RNA synthesis assays were performed either lacking metal cations, or with either Mg^{2+} or Mn^{2+} included at a range of concentrations from 1 mM to 16 mM. Following the reaction, RNA products were treated with calf intestinal phosphatase (CIP) to improve the signal to background ratio near the bottom of the gel. It should be noted that the phosphatase treatment caused RNA transcripts $\leq$6–10 nt to migrate differently from the markers (because they lack 5′ phosphate) and instead these bands migrated between the 8 and 10 nt markers. In the absence of metal cations, no RNA synthesis products were detected (Fig. 3A and B, lane 4). Increasing the concentration of Mg^{2+} promoted all RNA synthesis activities, with the highest levels of *de novo* RNA synthesis and 3′ extension being observed at 8 mM $MgCl_2$ (Fig. 3A). There was a change in the pattern of nucleotide addition during 3′ extension, with higher Mg^{2+} concentrations increasing the frequency of two and three nucleotide additions (compare lane 7 with lanes 8 and 9). However, aside from this difference, the relative levels of *de novo* initiation, elongation, and 3′ extension were not differentially affected by varying Mg^{2+}. Addition of Mn^{2+} to the reactions instead of Mg^{2+} also enabled *de novo* initiation and 3′-extension (Fig. 3B, lanes 5–7), demonstrating that RSV RdRp could use this as an alternative metal cation for both processes, but at higher concentrations (8 and 16 mM) Mn^{2+} was inhibitory (Fig. 3B, lanes 8 and 9). Whereas varying Mg^{2+} concentration had only subtle or negligible effects on the different RdRp RNA synthesis activities, this was not the case for Mn^{2+}. Inclusion of Mn^{2+} at the lowest concentration tested (1 mM) supported relatively efficient initiation of *de novo* RNA synthesis, resulting in accumulation of products migrating at 8–10 nt, and the levels of these products were only increased approximately 2–3 fold as the concentration of Mn^{2+} was increased to 4 mM. However, comparison of the intensity of bands migrating at 8–10 nt with the 21 nt band indicated that while Mn^{2+} supported initiation of RNA synthesis at a relatively high level, it was inefficient at supporting RNA synthesis elongation (Fig. 3, compare panels A and B). In contrast, at the lowest concentrations tested (1 and 2 mM) Mn^{2+} supported only a relatively low level of 3′ extension, but the efficiency of 3′ extension increased substantially as the concentration of Mn^{2+} was increased from 2 to 4 mM, similarly to the results obtained with Mg^{2+}. Thus, the RdRp performed the activities of 3′ extension and *de novo* RNA synthesis differently depending on the identity and concentration of metal cation available, with lower concentrations of Mn^{2+} favoring *de novo* initiation *versus* 3′ extension.

NaCl, DMSO and glycerol, which have previously shown to affect activities of other RdRps (Chen and Patton, 2000; Paul et al., 1998), were examined to determine if they had an effect on the RSV RdRp. None of these factors affected the relative levels of 3′ extension and *de novo* RNA synthesis. NaCl was found to be inhibitory to all RNA synthesis, particularly at concentrations $\geq$100 mM, glycerol was found to slightly enhance RNA synthesis, and DMSO had no detectable effect (data not shown).

The first 12 nt of the trc promoter are sufficient for de novo RNA synthesis

Having found that 3′ extension and *de novo* RNA synthesis occur under each of the experimental conditions that were tested,

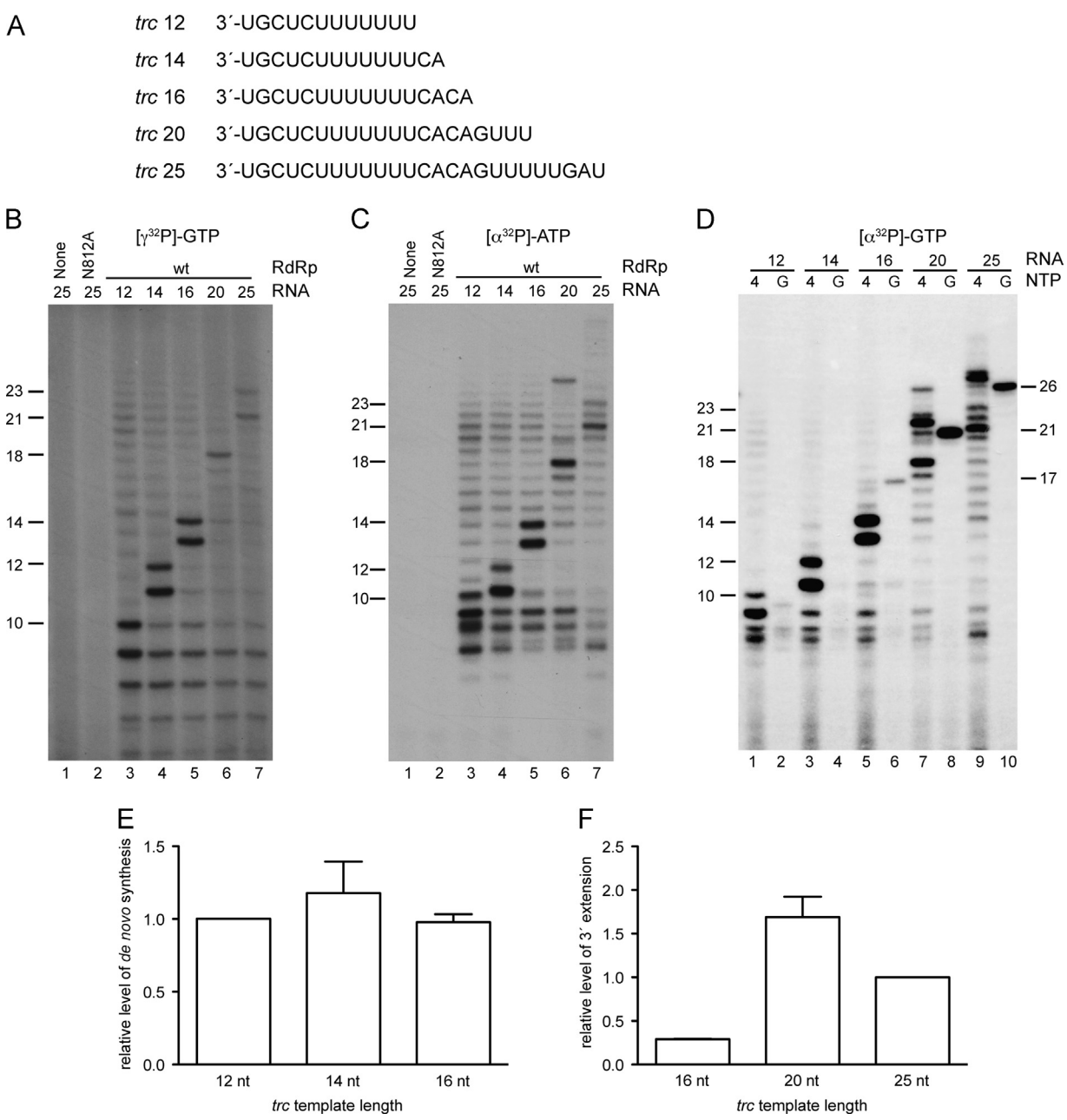

Fig. 4. Impact of *trc* template length on RSV RdRp activities. (A) Templates representing the 3′ 12, 14, 16, 20 or 25 nt of the *trc* promoter. (B) RNA templates illustrated in panel A were combined with standard buffer, but containing 250–500 μM each NTP (depending on the experiment) and [γ-^{32}P] GTP, and incubated for 2–5 h (depending on the experiment). (C) RNA templates were incubated for 30 min in standard RNA synthesis buffer, including [α-^{32}P] ATP. (D) RNA templates were incubated for 30 min in standard RNA synthesis buffer containing [α-^{32}P] GTP and either all four NTPs (4) or GTP alone (G) and wt RdRp. In panels B and C, lanes 1 and 2 are negative controls in which either no RdRp or RdRp containing the N812A substitution in the L protein was included in the reaction, respectively. The sizes of the RNA products were determined by comparison with the markers shown in Figs. 2 and 3. (E) Bar chart showing the levels of *de novo* RNA synthesis from each of the templates as measured by quantification of [γ^{32}P] GTP containing RNA products as shown in panel B, and [α-^{32}P] ATP products as shown in panel C. For quantification, all detectable bands, not including the stuttering products, from the 12, 14, and 16 nt templates were measured. Each bar represents the mean and standard error of three or four independent experiments. The data from each experiment were normalized to the product from the 12 nt template, which was set to a value of 1. Note that it was not possible to accurately quantify the levels of *de novo* RNA synthesis for the 20 and 25 nt templates because the signal is distributed between many faint bands. (F) Bar chart showing the levels of 3′ extension from each of the templates as measured by quantification of [α-^{32}P] GTP containing RNA in reactions containing GTP as the only NTP, as shown in panel D, lanes 2, 4, 6, 8 and 10. Each bar represents the mean and standard error of three independent experiments. The data from each experiment were normalized to the product from the 25 nt template, which was set to a value of 1.

we examined the contribution of different regions of the *trc* promoter to the two different RNA synthesis activities. Previous studies had indicated that there was a core promoter element located within nucleotides 1–12 of the *le* and *trc* promoter regions (Cowton and Fearns, 2005; Fearns et al., 2002; Peeples and Collins, 2000). However, it was not known if nucleotides 1–12 contain all the signals required to direct initiation of RNA synthesis, or if sequence beyond the first 12 nt impacts RdRp behavior during *de novo* RNA synthesis. To investigate this, templates consisting of the 3′ terminal 12, 14, 16, 20 and 25 nt of *trc* sequence were analyzed (Fig. 4A). RNA synthesis reactions were performed that included templates together with all four NTPs and [γ-^{32}P] GTP to allow analysis of RNA initiated from position +3, the dominant *de novo* synthesized product (Fig. 4B). The 12 nt template yielded abundant RNA synthesis products, with a dominant band at 10 nt, which would correlate with RNA initiated at position 3 and extended to the end of the template. Increasing the length of the template to 14 and 16 nt had no significant effect on the levels of

products, indicating that nucleotides 13–16 are not required for promoter activity (Fig. 4B, lanes 3–5; Fig. 4E). Further increases in template length appeared to slightly suppress *de novo* RNA synthesis (Fig. 4B, lanes 6 and 7). Similar results were obtained in reactions containing [α^{32}P] ATP, which would allow detection of RNA initiated from +1 and +3 (Fig. 4C), and [α^{32}P] GTP, which would allow detection of *de novo* RNA synthesis from +1 and +3 and 3′ extension activity (Fig. 4D, lanes 1, 3, 5, 7, and 9). These data show that the promoter for *de novo* RNA synthesis is contained within the 3′ 12 nt of *trc*.

It was noticeable that the 12, 14 and 16 nt templates each yielded a ladder of bands that were longer than the input templates (Fig. 4B and C, lanes 3–5; Fig. 4D, lanes 1, 3, and 5). The relative intensities of these bands were increased if [α^{32}P]-ATP was used as a label instead of [α^{32}P]-GTP, indicating that these longer products arose as a consequence of additional A residues being inserted into the products (Fig. 4, compare panels C and D). As RSV RdRp stuttering at a U_6 tract has been reported previously (Garcia-Barreno et al., 1990), it seemed likely that these products are the result of RdRp stuttering on a U_7 stretch that extends from nucleotides 6–12 of the *trc* promoter. The levels of stutter products decreased as the length of the template was increased to 16 nt, but remained at a detectable level. We hypothesized that the RSV RdRp might be particularly prone to stuttering within the promoter, before it had undergone conformational changes that enabled it to enter a stable elongation mode. To examine if this is the case, we analyzed data from next generation sequencing experiments performed on poly A enriched RNA isolated from RSV infected cells and determined the frequency of one or more nucleotide insertions at this *trc* U_7 tract. This analysis showed that 1.25% of *trc* and *tr* containing RNA transcripts contained additional A and U residues. A similar or slightly higher stuttering frequency was found at the other U_7 tracts within the RSV genome ($\leq$3.84%) (Table 1). A higher stuttering frequency was also found in cellular mRNAs with similarity to the RSV G gene (5%). These findings suggest that the RSV RdRp is not especially prone to stuttering at the *trc* U_7 tract during RNA replication in infected cells, or that if it does stutter at this site, it does not continue to elongate the RNA.

More than 16 nt of trc sequence are required for efficient 3′ extension

As described above, 3′-extension involves base-pairing of nucleotides 1 and 2 with nucleotides 13 and 14 to form a hairpin structure that primes templated extension, with between 1 and 3 residues typically added (Fig. 1B). To examine the effect of template length on 3′ extension, reactions were performed using the same templates as those described above, but in this case GTP (including [α^{32}P] GTP) was the only NTP included (Fig. 4D, lanes 2, 4, 6, 8 and 10). These reaction conditions would allow addition of the first nucleotide by 3′ extension, but would not support *de novo* RNA synthesis. As anticipated no signal corresponding to 3′ nucleotide addition was observed for the *trc* 12 or 14 nt RNAs (Fig. 4D, lanes 2 and 4), but products one residue longer than the input RNA were observed for the *trc* 16, 20 and 25 nt RNAs (Fig. 4D, lanes 6, 8 and 10), consistent with 3′ extension occurring by back-priming. The frequency of 3′ extension increased with templates $\geq$20 nt (Fig. 4D, compare lanes 6 and 8; Fig. 4F), which indicated that either the longer RNA molecules or specific nucleotides beyond position 16 enhanced the process. In addition, whereas the 25 nt template yielded 3′ extension products that were predominantly 26, 27 and 28 nt in length, the 20 nt template yielded relatively high levels of a product that was 26 nt in length and labeled with GTP and ATP, consistent with the RdRp having performed 3′ extension to the end of the template (Fig. 4C, lane 6; Fig. 4D, lane 7). This result suggested that nucleotides between positions 21 and 25 affect the ability of the RdRp to cease 3′ extension after addition of one to three nucleotides. Thus, these data show that the 3′ 16 nt of *trc* are sufficient for 3′ extension to occur. However, 20 nt allow significantly more efficient 3′ extension activity, and a sequence beyond position 20 modulates the RdRp to limit the number of nucleotides that are added.

The le promoter has the capability to direct 3′ extension in vitro

The *le* promoter, located at the 3′ end of the genome, has a high degree of sequence similarity to *trc* (Mink et al., 1991). However, sequence analysis of RNA from RSV infected cells had found no evidence of nucleotides added by back-priming (Noton et al., 2012). This was a surprising finding given that the *le* has the potential to form a stronger secondary hairpin structure than *trc* (Fig. 5A). Therefore, we examined if the difference in 3′ extension frequency on *le* and *trc* during infection was due to a difference in the ability of the RdRp to add nucleotides to *le* and *trc* sequences. First, we examined if the RdRp could add nucleotides to the 3′ end of the *le*. Based on the predicted hairpin structure, it was anticipated that if 3′-extension occurred, an A residue would be added first followed by a C residue. A reaction was performed containing a *le* 1–25 nt RNA, all four NTPs and an [α-^{32}P] ATP label. A series of products were detected in reactions containing wt RdRp, which included products $\geq$26 nt in length, consistent with back-priming and 3′ extension (Fig. 5B, lane 4). To confirm that these longer products were due to the predicted back-priming

Table 1
Stuttering frequency in RNA transcripts from RSV infected cells.

Genome location of U tract[a]	Expected RNA product with 5′ and 3′ flanking sequence[b]	Total number of sequences	Sequences with additional A residues	Stuttering frequency[c]
le (37–43)	UGCAUAAACC**AAAAAAA**UGGGGCAAAU	2119	23	1.08
N (1546–1552)	AAAAUCCUAC**AAAAAAA**UGCUAAAAGA	102,910	1013	0.98
P-M (3237–3243)	AUAUAGUUAC**AAAAAAA**GGAAAGGGUG	4059	68	1.67
M (3726–3732)	UAGUAACAUC**AAAAAAA**GUCAUAAUAC	388,235	2064	0.53
G (5297–5303)	CCAAGCCCAC**AAAAAAA**CCAACCCUCA	711586	27344	3.84
F (6028–6034)	CAACAAUGCC**AAAAAAA**CCAAUGUAAC	205,158	3196	1.55
L (12306–12312)	UACACAAGAG**AAAAAAA**CAAUGCCAGU	18,763	387	1.86
L (14687–14693)	ACCCUAUAAC**AAAAAAA**GGAAUUAAUA	10,006	57	0.57
trc (6–12)	5′–ACGAG**AAAAAAA**GUGUCAAAAA[d]	160	2	1.25

[a] The location is given for the nucleotide position of the U_7 tract in the RSV A2 genome sequence, except for the *trc* U_7 tract, which is given as its position in the RSV A2 antigenome. Note that the U_6 tract that lies at nucleotides 6–11 of the *le* promoter was also included in the analysis.
[b] The A tract is indicated in boldface type, with flanking sequences included, the underlined sequence was used for the search.
[c] Stuttering frequency is the number of transcripts with additional A residues as a percentage of the total sequences.
[d] Sequence term searched for was “ACACUUUUUUUCUCG”.

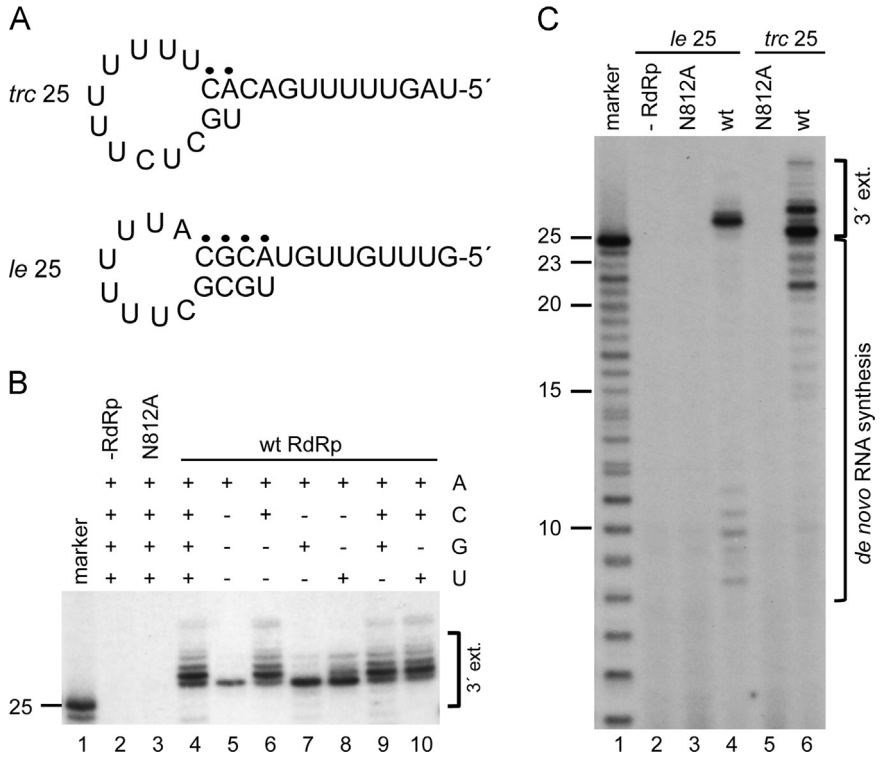

Fig. 5. The 3′ 25 nt of *le* support 3′-template extension *in vitro*. (A) Potential back-priming structures of RNAs representing the 3′ 25 nt of the *trc* and *le* regions, as indicated. In the case of *trc*, residues 1 and 2 can base-pair with residues 13 and 14 (indicated with black dots) or residues 15 and 16, whereas *le* residues 1–4 can base-pair with residues 13–16 (indicated with black dots). (B) RNA consisting of nt 1–25 of *le* sequence was incubated for 30 min with standard buffer and either all four NTPs or various combinations of NTPs, as indicated, in the presence of [α-^{32}P] ATP. Control reactions containing no RdRp or mutant RdRp containing the N812A substitution in the L protein are shown (lanes 2 and 3). Lane 1 is a 25 nt size marker. (C) Comparison of 3′-terminal extension activities of *le* and *trc* RNAs. Indicated RNA was incubated for 30 min with standard buffer containing all four NTPs and [α-^{32}P] CTP.

structure shown in Fig. 5A, reactions were performed containing either [α-^{32}P] ATP alone or together with different combinations of NTPs (Fig. 5B, lanes 5–10). This analysis indicated that ATP alone could facilitate extension by one nucleotide (Fig. 5B, lane 5), and inclusion of ATP and CTP could reconstitute the same pattern of products as all four NTPs (Fig. 5B, lanes 4 and 6). This result was consistent with addition of ACAA to *le* 25, as would be predicted. There was also evidence that sequence consisting of As and Us could be added (Fig. 5B, lane 8). This could be due to misincorporation of U in place of C during 3′ extension. Having found that the *le* could direct back-priming, the relative efficiencies of 3′ extension of the *le* and *trc* RNAs were examined. To accomplish this, reactions were performed containing all four NTPs, including [α-^{32}P] CTP. CTP is the second nucleotide added to the 3′ end of *le* and the third nucleotide added to the 3′ end of *trc*. It can also be the first nucleotide added to the 3′ end of *trc* if RNA folds into a structure with nucleotides 1 and 2 base-pairing with nucleotides 15 and 16. Because C is added in a different sequential order in *le versus trc*, this analysis does not allow the total levels of 3′ extension to be directly compared, but it represents the most sensitive method for measuring 3′ extension and allows an approximate indication of relative efficiencies. The results showed that despite its inherently weaker RNA hairpin structure, the *trc* RNA was equally or more efficient at 3′-template extension than *le* (Fig. 5C, compare lanes 4 and 6). This result shows that the RNA sequence affects the efficiency of 3′-extension, and that the frequency is not directly correlated to the inherent stability of the stem loop structure. However, the fact that 3′ extension could occur on the *le* sequence in this assay, but apparently does not occur in infected cells, suggests that during infection, the ability of the RdRp to perform 3′ extension is controlled by the presence of a factor or factors missing from the *in vitro* assay.

Discussion

The ability of the RSV RdRp to have two distinct RNA synthesis activities at the *trc* promoter indicates that it can adopt different conformations when it encounters a promoter sequence. The experiments described here begin to provide some light on which factors do, and do not determine which activity the RdRp will engage in.

As described above, RdRps require metal cations to catalyze RNA synthesis and typically Mg^{2+} ions fulfill this role. There is evidence that many RdRps also have a non-catalytic Mn^{2+} binding site (Butcher et al., 2001; Ferrer-Orta et al., 2004; Hansen et al., 1997; Malet et al., 2007; Ng et al., 2004; Poranen et al., 2008; Tao et al., 2002; Wright et al., 2012; Yap et al., 2007). In the presence of either Mg^{2+} or Mn^{2+}, the catalytic and non-catalytic sites can potentially be occupied by whichever metal ion is available. Given that Mg^{2+} and Mn^{2+} have different chemical properties, and can have different effects on RdRp structure, it is not surprising that a range of complex effects have been described when Mg^{2+} is substituted with Mn^{2+} in RNA synthesis reactions (Arnold et al., 1999, 2004; Butcher et al., 2001; Palmenberg and Kaesberg, 1974; Ranjith-Kumar et al., 2002a, 2002b; Shim et al., 2002). While these phenomena might represent abnormal RdRp activities that would not occur in the Mg^{2+} rich cellular environment, it had been speculated that a subset of viral RdRp bound to Mn^{2+} could have functional significance, by enabling repair of viral genomes, or increasing viral diversity (Ranjith-Kumar et al., 2002a, 2002b; Selisko et al., 2012). In this study we asked a simple question, specifically whether divalent cation identity could influence the relative levels of 3′ extension *versus de novo* initiation (Fig. 3). At low concentrations of Mn^{2+}, *de novo* initiation was stimulated relative to 3′ extension (Fig. 3D). This indicated that the

ability of the RdRp to associate with the *trc* sequence in a particular orientation and form a complex capable of RNA synthesis was altered by the identity of the cation. However, although Mn^{2+} could stimulate *de novo* initiation, compared to Mg^{2+} it was inefficient at supporting elongation of *de novo* initiated RNA at any of the tested concentrations (Fig. 3B). These results suggest that in infected cells, RdRp binding to Mn^{2+} prior to interacting with the promoter may cause the RdRp to adopt a conformation that favors *de novo* initiation rather than 3′ extension. However, the results also suggest that if this were to happen, Mn^{2+} would need to be replaced by Mg^{2+} to allow efficient elongation of the *de novo* synthesized RNA.

Previous studies had indicated that the 3′ 12 nucleotides would be sufficient for RNA synthesis to occur (Cowton and Fearns, 2005). The data presented in Fig. 4 confirm that nucleotides 1–12 contain a fully functional promoter and show that inclusion of additional sequence did not significantly augment promoter activity. The *trc* sequence downstream of nt 12 is highly conserved between the different subgroups of RSV, and it is likely that *trc* sequence downstream of nt 12 is important for genome synthesis. However, the data presented here and in previous work (McGivern et al., 2005) suggest that this region of the promoter fulfills a function that occurs after RNA synthesis initiation, most likely elongation and/or encapsidation. In this *in vitro* assay, promoter activity appeared to be inhibited by inclusion of 20 and 25 nt of *trc* sequence. This was not simply due to formation of secondary structure in the promoter sequence, as nucleotides 1–14 would be sufficient for this to occur. Possibly the more efficient 3′ extension that occurred with the longer templates diverted the RdRp away from *de novo* synthesis. This may not happen in the context of an infected cell, where other factors likely come into play to regulate RdRp activity between *de novo* RNA synthesis and 3′ extension.

Different lengths of *trc* template differed slightly in the quality of the products that they generated. The 12, 14, and 16 nt templates had a significant level of premature termination one nucleotide prior to the template end, and the 25 nt template generated a relatively high proportion of product that terminated two nucleotides prior. This indicated that the template sequence and/or length could impact the ability of the RdRp to insert nucleotides opposite to the 5′ terminus, which might be similar to findings with positive strand RNA virus RdRps (Tayon et al., 2001). In addition, the 12, 14 and 16 nt templates gave rise to products consistent with RdRp stuttering at the U_7 tract present at nucleotides 6–12. The levels of products generated by stuttering diminished with increasing lengths of template, likely because this provided an RNA sequence for the RdRp to continue moving along. RNA seq analysis of RNA from RSV infected cells indicated that the frequency of insertion at this site was 1.25%, a similar frequency as at other U_7 tracts in the RSV genome, and lower than at U_7 tracts in cellular RNA. This indicates that the RSV RdRp does not stutter at a frequency above the background stuttering of the reverse transcriptase used to generate cDNA for RNA-seq analysis. In addition, in previous work in which replicative RNA from minigenome transfected or RNA infected cells was analyzed by primer extension analysis, we did not detect stuttering at the *trc* promoter at a level comparable to that observed in this *in vitro* assay (Noton et al., 2012; Tremaglio et al., 2013). This can suggest that the RSV RdRp is more error prone in the *in vitro* assay than it is in cells. Alternatively, stuttering might cause the RdRp–RNA complex to dissociate, resulting in abortive transcripts that would not have been detected in the RNA seq or primer extension analyses. Interestingly, the products generated by RdRp stuttering tended to reach a maximum length of ~21 to 25 nt (Fig. 4A and B), the same length at which the RdRp releases templated RNA initiated from both the +1 and +3 sites *in vitro* (Fig. 2, panels B and C) and RNA initiated from the +3 site in infected cells (Tremaglio et al., 2013). This finding suggests that following initiation at the promoter, the RSV RdRp has a propensity to release the RNA transcript after approximately 21–25 nt, regardless of the sequence of the product. It seems likely that in the context of an infection, encapsidation by N protein before the RdRp has synthesized 21–25 nt stabilizes the RdRp, allowing it to elongate further.

The results shown in Figs. 4D and 5 indicate that the RNA sequence affects the efficiency and accuracy of 3′ extension. Although base-pairing can potentially occur between nucleotides 1 and 2, and 13 and 14, the data presented in Fig. 4D show that the RdRp requires more than 16 nt of *trc* RNA for back-priming and 3′ extension to be efficient. It is possible that the extra RNA is required for the RdRp to bind and form a stable complex. Sequence downstream of the base-pairing site also appeared to play some role in governing how many nucleotide additions were made, as the 20 nt *trc* RNA tended to yield 3′ extension products that were extended to the end of the RNA with slightly greater frequency than the 25 nt *trc* RNA. It should be noted that the 25 nt *trc* RNA does not completely recapitulate the events that occur in infected cells, as this RNA enabled base-pairing of nts 1 and 2 with nts 15 and 16, in addition to nts 13 and 14 (*e.g.* Fig. 5C), whereas analysis of *trc* containing RNA from infected cells indicated that 3′ extension involved base pairing with nts 13 and 14 only. It is possible that additional RNA sequence and/or other factors contribute to the accuracy of 3′ extension in infected cells. The efficiency of 3′ extension was not increased by using *le* sequence, which had greater potential to adopt a stable secondary structure. This suggests that the RdRp is largely responsible for folding the RNA into the secondary structure required for back-priming to occur, which is consistent with the fact that the structure within *trc* would be expected to be weak or non-existent in RNA alone. In addition, the pattern of 3′ extension was similar with *le* and *trc* sequences, with addition of two nucleotides generally being dominant. This was the case, even though *trc* and *le* had a number of nucleotide differences in the region where the 3′ end of the RNA folded into a secondary structure and the nucleotides added were different. Together, these findings suggest that 3′ extension is affected by the RNA sequence, but that the RdRp itself plays a key role in forming the secondary structure required and determining how many nucleotides will be added.

There is clearly a difference between the efficiency of 3′ extension *in vitro versus* infected cells, with it being the dominant event at the *trc* promoter *in vitro* and occurring at the *le* promoter in this *in vitro* assay, but not in infected cells (Noton et al., 2012). The most likely explanation for why RNA would or would not be modified by 3′ extension is that formation of the secondary structure required for back-priming is dependent on the RNA not being encapsidated. In this *in vitro* assay, none of the RNA was encapsidated, which could have increased the efficiency of 3′ extension to a frequency that was much greater than in infected cells. If encapsidation is key, there are at least two possible explanations why the *le* is not modified by 3′ extension. First, it is possible that the *trc* RNA that is modified in RSV infected cells is not within the antigenome, but rather is part of an L-trc readthrough mRNA. If an L-trc readthrough mRNA were generated, it would not be expected to be encapsidated and this could allow the end of the *trc* sequence to fold into the back-priming structure. Because RSV is not ambi-sense, no corresponding RNA would exist for *le* containing RNA. However, the RSV L gene end sequence signals efficient termination, with no evidence for readthrough in a minigenome assay (Cartee et al., 2003), and so there is no strong evidence that L-trc mRNA exists in infected cells. A second explanation is that the *trc* RNA might sometimes be unencapsidated, whereas the *le* might always, or almost always be encapsidated. We have previously suggested that back-priming activity at

the *trc* promoter might be a mechanism for negatively regulating promoter activity under conditions of low N protein. This might function to prevent genome synthesis from occurring until there is a sufficiently high N protein concentration. Ensuring that genome synthesis only occurs under conditions of high N protein concentration might be necessary to avoid generation of unencapsidated RNA complementary to mRNA, which could strongly activate dsRNA sensors and inhibit mRNA translation. In contrast, it might not be so important for antigenome RNA to be concurrently encapsidated, and so a similar regulatory control might not need to exist at the *le* promoter.

In summary, the data presented here show that the *de novo* RNA synthesis and 3′ extension activities of the RSV RdRp are differentially affected by environmental conditions. They also reveal new information about what RNA sequences are required for these events to occur, and provide some insight into how 3′ extension might be controlled. This information increases our understanding of the properties of the RdRp–*trc* RNA complexes and may be helpful for future functional and structural analyses of the RSV RdRp.

Materials and methods

RSV RdRp purification and RNA synthesis assays

The RSV L and P proteins were expressed in insect cells using recombinant baculovirus and the L/P complex was purified as described previously (Noton et al., 2012). RNA synthesis was reconstituted *in vitro* using a similar approach as described previously (Noton et al., 2012; Tremaglio et al., 2013), but with some modifications. Templates consisted of PAGE purified RNA oligonucleotides corresponding to various lengths of the *trc* or nt 1–25 of the *le* promoter, as indicated in the text. RNA (2 μM) was combined with the purified L/P complex (containing ~200 ng of L protein) in RNA synthesis buffer. The standard reaction buffer was 50 mM Tris HCl pH 7.4, 8 mM $MgCl_2$, 5 mM DTT, 10% glycerol, 1 mM each NTP, and 10 μCi of either [α^{32}P], or [γ-^{32}P] ATP or GTP in a final volume of 50 μl. Reactions were incubated at 30 °C for the indicated lengths of time, followed by incubation at 90 °C for 3 min to inactivate the RdRp, and cooled on ice. With the exception of the experiment shown in Fig. 2A, reactions involving [α^{32}P] NTPs were combined with 20 U calf intestinal alkaline phosphatase (NEB), and incubated at 37 °C for 1 h. Reactions involving [γ-^{32}P] NTPs were incubated with 1 U of terminator exonuclease (Epicentre) and further incubated for 1 h at 30 °C, heated to 90 °C for 3 min and cooled briefly on ice, to remove template RNA that had become labeled by kinase activity that is present in the L/P preparation. These reactions were then combined with 7.5 μl 10% SDS, 0.5 μl 500 mM EDTA and 10 μg proteinase K and incubated at 45 °C for 45 min. RNA was isolated by phenol–chloroform extraction and ethanol precipitation and then resuspended in water and diluted in an equal volume of stop buffer (deionized formamide containing 20 mM EDTA, bromophenol blue, xylene cyanol). One-third of the reaction products were analyzed by electrophoresis on a 20% polyacrylamide gel containing 7 M urea in Tris–borate–EDTA buffer, followed by autoradiography. The nucleotide lengths of the RNA products were determined by comparison with a molecular weight ladder generated by alkaline hydrolysis of a [γ-^{32}P] end-labeled RNA oligonucleotides representing the anticipated 23 and/or 25 nucleotide *tr* RNA products. The data were quantified by analyzing TIF images of the autoradiograms using Quantity One software. To ensure that the values obtained were in the linear range, a standard curve was generated by preparing a two-fold dilution series of one of the markers. This standard was included on all scans.

Sequence analysis of RSV RNA

RNA was isolated from A549 or HEp-2 cells infected with RSV strain A2 using an RNeasy kit (Qiagen). Poly A enriched RNA was fragmented and reverse transcribed. The cDNA fragments were sequenced using an Illumina HiSeq platform to generate ~50 million 100 bp paired end reads for each sample. Sequence reads were aligned to either a canonical list of human transcripts (215,621 transcripts) or the RSV-A2 genome using Bowtie 2 with default parameters (Langmead and Salzberg, 2012). The output file of sequence reads mapping to the RSV genome was converted from BAM to SAM format and the resulting SAM files were searched for sequences that exactly matched the target run of sequences or for those that matched, but with any number of additional A nucleotides inserted, as indicated in the *Results* section. As a control we used this approach to examine the results of mapping to the human genome looking at poly A rich sequences that matched a similar sequence to that of the RSV G glycoprotein. The data shown in Table 1 were derived from RNA isolated from A549 cells; similar results were obtained for RNA isolated from HEp-2 cells.

Acknowledgments

R. F. would like to thank Dominique Garcin for helpful discussions regarding the potential significance of RSV 3′ extension. This research was funded by NIH Grant R01AI074903 to R.F. and Boston University School of Medicine. The funders had no involvement in the study design, data interpretation or writing of this article.

References

Albertini, A.A., Wernimont, A.K., Muziol, T., Ravelli, R.B., Clapier, C.R., Schoehn, G., Weissenhorn, W., Ruigrok, R.W., 2006. Crystal structure of the rabies virus nucleoprotein–RNA complex. Science 313, 360–363.
Arnold, J.J., Ghosh, S.K., Cameron, C.E., 1999. Poliovirus RNA-dependent RNA polymerase (3D(pol)). Divalent cation modulation of primer, template, and nucleotide selection. J. Biol. Chem. 274, 37060–37069.
Arnold, J.J., Gohara, D.W., Cameron, C.E., 2004. Poliovirus RNA-dependent RNA polymerase (3Dpol): pre-steady-state kinetic analysis of ribonucleotide incorporation in the presence of Mn^{2+}. Biochemistry 43, 5138–5148.
Bakker, S.E., Duquerroy, S., Galloux, M., Loney, C., Conner, E., Eleouet, J.F., Rey, F.A., Bhella, D., 2013. The respiratory syncytial virus nucleoprotein–RNA complex forms a left-handed helical nucleocapsid. J. Gen. Virol. 94, 1734–1738.
Butcher, S.J., Grimes, J.M., Makeyev, E.V., Bamford, D.H., Stuart, D.I., 2001. A mechanism for initiating RNA-dependent RNA polymerization. Nature 410, 235–240.
Cartee, T.L., Megaw, A.G., Oomens, A.G., Wertz, G.W., 2003. Identification of a single amino acid change in the human respiratory syncytial virus L protein that affects transcriptional termination. J. Virol. 77, 7352–7360.
Chen, D., Patton, J.T., 2000. De novo synthesis of minus strand RNA by the rotavirus RNA polymerase in a cell-free system involves a novel mechanism of initiation. RNA 6, 1455–1467.
Cowton, V.M., Fearns, R., 2005. Evidence that the respiratory syncytial virus polymerase is recruited to nucleotides 1 to 11 at the 3′ end of the nucleocapsid and can scan to access internal signals. J. Virol. 79, 11311–11322.
Cowton, V.M., McGivern, D.R., Fearns, R., 2006. Unravelling the complexities of respiratory syncytial virus RNA synthesis. J. Gen. Virol. 87, 1805–1821.
Fearns, R., Peeples, M.E., Collins, P.L., 2002. Mapping the transcription and replication promoters of respiratory syncytial virus. J. Virol. 76, 1663–1672.
Ferrer-Orta, C., Arias, A., Perez-Luque, R., Escarmis, C., Domingo, E., Verdaguer, N., 2004. Structure of foot-and-mouth disease virus RNA-dependent RNA polymerase and its complex with a template-primer RNA. J. Biol. Chem. 279, 47212–47221.
Garcia-Barreno, B., Portela, A., Delgado, T., Lopez, J.A., Melero, J.A., 1990. Frame shift mutations as a novel mechanism for the generation of neutralization resistant mutants of human respiratory syncytial virus. EMBO J. 9, 4181–4187.
Green, T.J., Zhang, X., Wertz, G.W., Luo, M., 2006. Structure of the vesicular stomatitis virus nucleoprotein–RNA complex. Science 313, 357–360.
Hansen, J.L., Long, A.M., Schultz, S.C., 1997. Structure of the RNA-dependent RNA polymerase of poliovirus. Structure 5, 1109–1122.
Jung, J., Lifland, A.W., Zurla, C., Alonas, E.J., Santangelo, P.J., 2013. Quantifying RNA-protein interactions *in situ* using modified-MTRIPs and proximity ligation. Nucleic Acids Res. 41, e12.

Kolakofsky, D., Roux, L., Garcin, D., Ruigrok, R.W., 2005. Paramyxovirus mRNA editing, the rule of six and error catastrophe: a hypothesis. J. Gen. Virol. 86, 1869–1877.
Langmead, B., Salzberg, S.L., 2012. Fast gapped-read alignment with Bowtie 2. Nat. Methods 9, 357–359.
Lifland, A.W., Jung, J., Alonas, E., Zurla, C., Crowe Jr., J.E., Santangelo, P.J., 2012. Human respiratory syncytial virus nucleoprotein and inclusion bodies antagonize the innate immune response mediated by MDA5 and MAVS. J. Virol. 86, 8245–8258.
Lindquist, M.E., Lifland, A.W., Utley, T.J., Santangelo, P.J., Crowe Jr., J.E., 2010. Respiratory syncytial virus induces host RNA stress granules to facilitate viral replication. J. Virol. 84, 12274–12284.
Malet, H., Egloff, M.P., Selisko, B., Butcher, R.E., Wright, P.J., Roberts, M., Gruez, A., Sulzenbacher, G., Vonrhein, C., Bricogne, G., Mackenzie, J.M., Khromykh, A.A., Davidson, A.D., Canard, B., 2007. Crystal structure of the RNA polymerase domain of the West Nile virus non-structural protein 5. J. Biol. Chem. 282, 10678–10689.
McGivern, D.R., Collins, P.L., Fearns, R., 2005. Identification of internal sequences in the 3′ leader region of human respiratory syncytial virus that enhance transcription and confer replication processivity. J. Virol. 79, 2449–2460.
Mink, M.A., Stec, D.S., Collins, P.L., 1991. Nucleotide sequences of the 3′ leader and 5′ trailer regions of human respiratory syncytial virus genomic RNA. Virology 185, 615–624.
Nair, H., Nokes, D.J., Gessner, B.D., Dherani, M., Madhi, S.A., Singleton, R.J., O'Brien, K.L., Roca, A., Wright, P.F., Bruce, N., Chandran, A., Theodoratou, E., Sutanto, A., Sedyaningsih, E.R., Ngama, M., Munywoki, P.K., Kartasasmita, C., Simoes, E.A., Rudan, I., Weber, M.W., Campbell, H., 2010. Global burden of acute lower respiratory infections due to respiratory syncytial virus in young children: a systematic review and meta-analysis. Lancet 375, 1545–1555.
Ng, K.K., Pendas-Franco, N., Rojo, J., Boga, J.A., Machin, A., Alonso, J.M., Parra, F., 2004. Crystal structure of norwalk virus polymerase reveals the carboxyl terminus in the active site cleft. J. Biol. Chem. 279, 16638–16645.
Noton, S.L., Fearns, R., 2011. The first two nucleotides of the respiratory syncytial virus antigenome RNA replication product can be selected independently of the promoter terminus. RNA 17, 1895–1906.
Noton, S.L., Cowton, V.M., Zack, C.R., McGivern, D.R., Fearns, R., 2010. Evidence that the polymerase of respiratory syncytial virus initiates RNA replication in a nontemplated fashion. Proc. Natl. Acad. Sci. U. S. A. 107, 10226–10231.
Noton, S.L., Deflube, L.R., Tremaglio, C.Z., Fearns, R., 2012. The respiratory syncytial virus polymerase has multiple RNA synthesis activities at the promoter. PLoS Pathog. 8, e1002980.
Palmenberg, A., Kaesberg, P., 1974. Synthesis of complementary strands of heterologous RNAs with Qbeta replicase. Proc. Natl. Acad. Sci. U. S. A. 71, 1371–1375.
Paul, A.V., van Boom, J.H., Filippov, D., Wimmer, E., 1998. Protein-primed RNA synthesis by purified poliovirus RNA polymerase. Nature 393, 280–284.
Peeples, M.E., Collins, P.L., 2000. Mutations in the 5′ trailer region of a respiratory syncytial virus minigenome which limit RNA replication to one step. J. Virol. 74, 146–155.
Poranen, M.M., Salgado, P.S., Koivunen, M.R., Wright, S., Bamford, D.H., Stuart, D.I., Grimes, J.M., 2008. Structural explanation for the role of Mn^{2+} in the activity of phi6 RNA-dependent RNA polymerase. Nucleic Acids Res. 36, 6633–6644.
Ranjith-Kumar, C.T., Gutshall, L., Kim, M.J., Sarisky, R.T., Kao, C.C., 2002a. Requirements for de novo initiation of RNA synthesis by recombinant flaviviral RNA-dependent RNA polymerases. J. Virol. 76, 12526–12536.
Ranjith-Kumar, C.T., Kim, Y.C., Gutshall, L., Silverman, C., Khandekar, S., Sarisky, R.T., Kao, C.C., 2002b. Mechanism of de novo initiation by the hepatitis C virus RNA-dependent RNA polymerase: role of divalent metals. J. Virol. 76, 12513–12525.
Samal, S.K., Collins, P.L., 1996. RNA replication by a respiratory syncytial virus RNA analog does not obey the rule of six and retains a nonviral trinucleotide extension at the leader end. J. Virol. 70, 5075–5082.
Santangelo, P.J., Lifland, A.W., Curt, P., Sasaki, Y., Bassell, G.J., Lindquist, M.E., Crowe Jr., J.E., 2009. Single molecule-sensitive probes for imaging RNA in live cells. Nat. Methods 6, 347–349.
Selisko, B., Potisopon, S., Agred, R., Priet, S., Varlet, I., Thillier, Y., Sallamand, C., Debart, F., Vasseur, J.J., Canard, B., 2012. Molecular basis for nucleotide conservation at the ends of the dengue virus genome. PLoS Pathog. 8, e1002912.
Shim, J.H., Larson, G., Wu, J.Z., Hong, Z., 2002. Selection of 3′-template bases and initiating nucleotides by hepatitis C virus NS5B RNA-dependent RNA polymerase. J. Virol. 76, 7030–7039.
Tao, Y., Farsetta, D.L., Nibert, M.L., Harrison, S.C., 2002. RNA synthesis in a cage – structural studies of reovirus polymerase lambda3. Cell 111, 733–745.
Tawar, R.G., Duquerroy, S., Vonrhein, C., Varela, P.F., Damier-Piolle, L., Castagne, N., MacLellan, K., Bedouelle, H., Bricogne, G., Bhella, D., Eleouet, J.F., Rey, F.A., 2009. Crystal structure of a nucleocapsid-like nucleoprotein–RNA complex of respiratory syncytial virus. Science 326, 1279–1283.
Tayon Jr., R., Kim, M.J., Kao, C.C., 2001. Completion of RNA synthesis by viral RNA replicases. Nucleic Acids Res. 29, 3576–3582.
Tremaglio, C.Z., Noton, S.L., Deflube, L.R., Fearns, R., 2013. Respiratory syncytial virus polymerase can initiate transcription from position 3 of the leader promoter. J. Virol. 87, 3196–3207.
Wright, S., Poranen, M.M., Bamford, D.H., Stuart, D.I., Grimes, J.M., 2012. Non-catalytic ions direct the RNA-dependent RNA polymerase of bacterial double-stranded RNA virus varphi6 from de novo initiation to elongation. J. Virol. 86, 2837–2849.
Yang, W., Lee, J.Y., Nowotny, M., 2006. Making and breaking nucleic acids: two-Mg^{2+}-ion catalysis and substrate specificity. Mol. Cell 22, 5–13.
Yap, T.L., Xu, T., Chen, Y.L., Malet, H., Egloff, M.P., Canard, B., Vasudevan, S.G., Lescar, J., 2007. Crystal structure of the dengue virus RNA-dependent RNA polymerase catalytic domain at 1.85-angstrom resolution. J. Virol. 81, 4753–4765.